ajfand SCHOLARLY, PEER REVIEWED
AFRICAN JOURNAL OF FOOD, AGRICULTURE, NUTRITION AND DEVELOPMENT
Volume 22 No. 7 September 2022
PUBLISHED BY AFRICAN SCHOLARLY SCIENCE COMMUNICATIONS TRUST
ISSN 1684 5374

*Afr. J. Food Agric. Nutr. Dev.* 2022; 22(7): 20993-21018 https://doi.org/10.18697/ajfand.112.21555

# ASSESSMENT ON IRRIGATION SYSTEM PERFORMANCE OF SUGARCANE FARM USING REMOTE SENSING AT LOWER OMO BASIN, ETHIOPIA

**Toma NS[1]*, Samuel DH[1] and A Tena[2]**

**Nigatu Toma**

*Corresponding author email: tomanigatu@yahoo.com

[1]Faculty of Water and Irrigation Engineering, Arbamich University, Ethiopia

[2]Water and Land Resource Center, Addis Ababa University, Ethiopia

CC BY NC ND

ajfand SCHOLARLY, PEER REVIEWED AFRICAN JOURNAL OF FOOD, AGRICULTURE, NUTRITION AND DEVELOPMENT Volume 22 No. 7 September 2022 PUBLISHED BY AFRICAN SCHOLARLY SCIENCE COMMUNICATIONS TRUST ISSN 1684 5374

**ABSTRACT**

This study was aimed at assessing the irrigation system performance at Omo Kuraz Sugar Cane Development Project using data from remote sensing and meteorological stations. To analyze the distribution of evapotranspiration over the treatment area, the SEBAL (Surface Energy Balance Algorithm) model was used to evaluate the evapotranspiration (ET) rate for sugarcane at the lower Omo River Basin. Surface energy balance algorithm input like NDVI, Land surface temperature, TOA albedo and emissivity was calculated from Land Lat 8 image using the ENVI software. The data were collected from the farm site meteorology station, and the calculated evapotranspiration rate was one of the inputs into irrigation system performance indicators model, along with actual field data gathered from irrigation delivery schedule, root depth of crop at each growth stage, soil moisture before and after irrigation, and water diverted to the field. The four pillars of irrigation system performance are over all consumed ratio, depleted fraction, evaporative fraction, and relative evapotranspiration. This study also examined system performance using four standard indicators; namely, adequacy, efficiency, reliability, and equity. These indicators were calculated using the SEBAL algorithm and data were classified based on satellite and irrigation application. The findings of this study revealed that the irrigation system performed poorly with all treatment fields being below the target performance indicator values (overall water consumption ratio, ep; depleted fraction, DF; evaporative fraction, ʌ and relative evapotranspiration, RET). The calculated crop water requirements using the SEBAL model and satellite data were not consistent with applied water. The findings from this study also showed that irrigation system performance indicator parameters were limited due to excessive water applied to the field. The study also revealed an acceptable range of RET (0.8, 0.9); however, the irrigation system's reliability was poor according to the results of field observations at the experimental site. This observation was due to the field receiving an excessive amount of water. These results and observations suggest that the irrigation agronomist should schedule irrigation water application based on crop water requirements to manage poor irrigation system performance.

**Key words:** Irrigation system performance, SEBAL model, Remote sensing, Landsat 8, lower Omo Basin

CC BY NC ND

ajfand SCHOLARLY, PEER REVIEWED AFRICAN JOURNAL OF FOOD, AGRICULTURE, NUTRITION AND DEVELOPMENT Volume 22 No. 7 September 2022 PUBLISHED BY AFRICAN SCHOLARLY SCIENCE COMMUNICATIONS TRUST ISSN 1684 5374

**Background of the Study**

It is argued that irrigation is a critical agricultural practice in semi-arid and arid regions to produce food, pasture, and fiber. Today, efficient water use and management are found major concerns in many countries, including Ethiopia. Irrigation water application was also the world's largest consumer of freshwater budget. However, irrigation application's cost-benefit has been questioned, owing primarily to poor water management of irrigation systems, particularly in water-scarce environments and problematic soil [1].

Evaluation of the performance of irrigation system in its current form is critical for designing and implementing any plan to achieve sustainable irrigation system management. The lack of objective data on agricultural situation in irrigated command areas at the desired spatial level was today's major problem for evaluation of irrigation system. Several studies in recent years have demonstrated the utility of remotely sensed data for generating information on total irrigated area and area under different crops [2]. In the same way, remotely sensed data may quickly reveal crop condition and crop production [3, 4]. This paper sought to demonstrate the potential of emerging technologies such as satellite remote sensing for generating and analyzing subjective data across space and time to achieve practical evaluation of agricultural situation and irrigation system performance of surface irrigation systems.

There are several types of irrigation system performance indicator parameters. Aside from water supply performance, one can differentiate agricultural, socioeconomic, and environmental performance [5, 6].The system of irrigation, system adequacy, equity, reliability, and efficiency in the environmental and socioeconomic arena for flexibility, sustainability, and productivity was used to assess the performance of agricultural irrigation systems, thus; this indicates that regardless of whether the irrigation project worked well in terms of agricultural production, it can be observed that water delivered to the field is connected to agricultural production [7]. When evaluating irrigation schemes from the standpoint of water budgeting services, performance objectives such as adequacy, efficiency, equity, and reliability are believed to be taken into account. In this regard, adequacy can be defined as a system's ability to meet demand, and it was the primary goal of a system. The ability to conserve resources is expressed by efficiency, and when an irrigation system provides a more than adequate supply, it cannot be considered efficient. Equity was also a measure of the impartiality of resource supply, and it can be defined as the spatial uniformity of the supply and demand components of irrigation application. Reliability, on the other hand, expresses the degree of temporal regularity of supply and demand by encapsulating the condition in which water is applied to the crop at the exact time [8].

CC BY NC ND

ajfand SCHOLARLY, PEER REVIEWED AFRICAN JOURNAL OF FOOD, AGRICULTURE, NUTRITION AND DEVELOPMENT Volume 22 No. 7 September 2022 PUBLISHED BY AFRICAN SCHOLARLY SCIENCE COMMUNICATIONS TRUST ISSN 1684 5374

The performance of irrigation systems was evaluated using multiple approaches, including mathematical equations, hydrological models, decision support systems, and remote sensing [8]. There are certain limitations to using a quantitative technique to evaluate irrigation system performance on a big scale, but it is more or less accurate [31]. However, modern remote sensing techniques were most successful in assessing irrigation system performance on a large irrigation scale [31]. GIS and remote sensing were used by some researchers in combination with a hydrological model [35, 36]. Both have drawbacks, according to another expert, but for large-scale irrigation fields, the remote sensing technique is strongly recommended [32].

The remote sensing equipment installed on landsat data continuity mission (LCDM) includes multichannel scanning radiometer OLI (operational land imager sensors) and a two-channel-IR radiometer TIRS (thermal infrared sensors). operational land imager (OLI) is a push-broom sensor with four mirrors and a 12-bit quantization. Operational land imager (OLI) captures data for the visible, near infrared, short wave infrared, and panchromatic spectral bands, as well as a panchromatic band [30].

Satellite remote sensing allows for the capture of information over a large area at regular intervals. The ability of satellite detection to manage agricultural and hydrological conditions on the land surface has changed dramatically in the last decade. In this regard, Engman and Gurney have previously presented some reviews on the advantages and disadvantages of remote sensing applications in the field of irrigation system management [9, 10, 11].The purpose of this study was to raise complaisance among scholars, consultants, and irrigation administrators about the advancement of remote sensing technology and to encourage them to participate in the public debate about how satellite data can be used and implemented in irrigation systems to mitigate the impact of water logging for sustainable development.

## MATERIALS AND METHODS

### Study Area

The Omo Give River Basin is located on the equator between latitude 3500'E and 3800'E and longitude 4030'N and 9030'N. The basin has an area of 79000 km$^2$ and its elevation ranges from 300 to 2800 meters. The Gibe River is known as the Omo River in its lower reaches, and the Omo River's general flow direction is southward towards the Turkan River in Kenya. It is a confined river basin that drains into Lake Turkana in Kenya, which serves as its southern boundary. The total mean yearly flow from the river basin was estimated to be approximately 16.6 billion cubic meters. Because of the

CC BY NC ND

ajfand SCHOLARLY, PEER REVIEWED AFRICAN JOURNAL OF FOOD, AGRICULTURE, NUTRITION AND DEVELOPMENT Volume 22 No. 7 September 2022 PUBLISHED BY AFRICAN SCHOLARLY SCIENCE COMMUNICATIONS TRUST ISSN 1684 5374

variability in topography, rainfall, and land use, the basin has complex hydrological processes.

The study area is the lower Omo-Gibe River Basin (Gibe IV catchment) located in the South Western highlands of Ethiopia. According to the field data gathered, the area receives rainfall for about nine to ten months per a year. The basin is located between 3400' to 3800'E latitude and 400' to 800'N longitude. This River Basin is also located around South Omo from Keffa.The geographical location of this study site is flat, with slopes of less than 2% in most places, which is ideal for mechanized commercial farming in general. This basin is characterized by diverse topographic features with elevations ranging from 380 m asl to 485 m asl. The command area annual rainfall is in the range of 661.4 mm, but the temperature over the project area varies from $190^0$C (July and August) to $33^0$C (February), while the wind speed ranges from 10.4 km/h to 15.5 km/h. The humidity ranges from 57 percent to 75 percent, and the sunshine hours range from 6.9 hours to 10.2 hours. The average monthly evapotranspiration ranges from 151 mm to 205 mm, with an annual value of 2 070 mm.

The gross command area of the main systems which is approximately 175,000 ha has been chosen to evaluate the performance of major irrigation systems (Fig. 1). In this regard, surface water is supplied by the irrigation system in the Omo Kuraz.

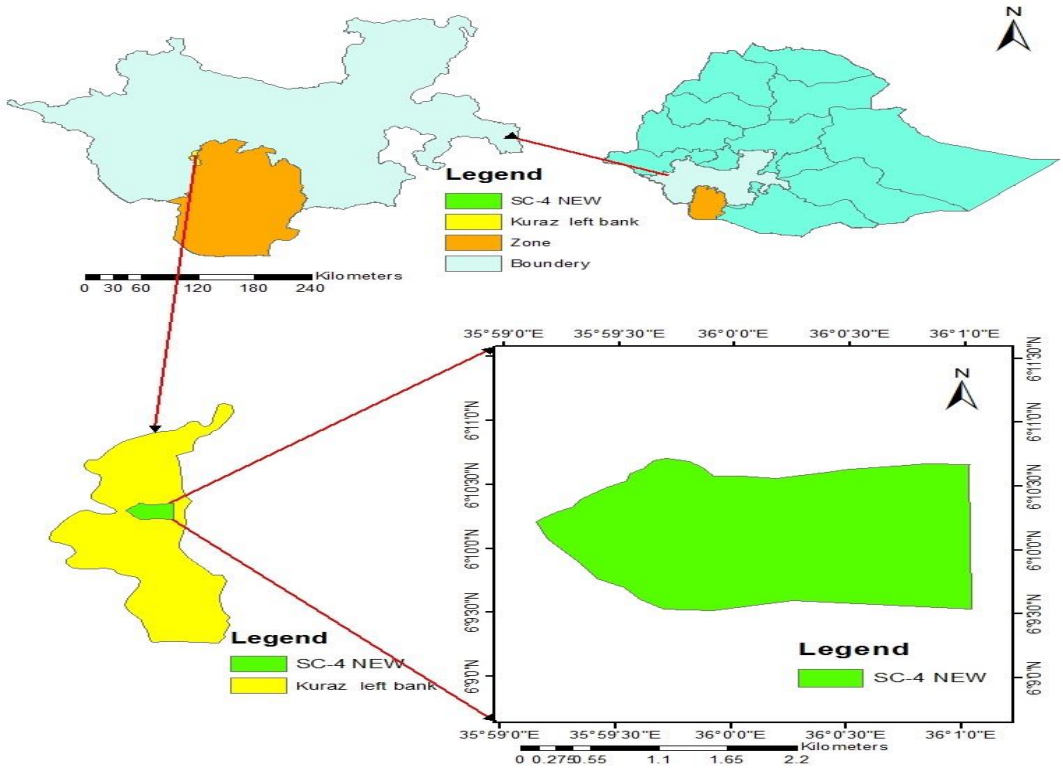


**Figure 1: Location Map of the study area**

CC BY NC ND

ajfand SCHOLARLY, PEER REVIEWED AFRICAN JOURNAL OF FOOD, AGRICULTURE, NUTRITION AND DEVELOPMENT Volume 22 No. 7 September 2022 PUBLISHED BY AFRICAN SCHOLARLY SCIENCE COMMUNICATIONS TRUST ISSN 1684 5374

**Experimental site**

The experiment was carried out in a sugarcane field. Four treatments from four stages of sugar cane development were selected. To measure the quantity of water diverted to the field and soil moisture, one treatment from the early stage (TE), one treatment from the planting stage (Tp), one treatment from the middle stage (TM), and one treatment from the harvesting stage (TH) were used. In addition, four furrows from each treatment were selected to assess soil moisture and measured the amount of water diverted to the field. The length of each furrow (0, 1/4,1/2,3/4) was used to measure the amount of water diverted to the field using a partial flume and soil moisture after and before irrigation using an auger. The experimental plot was situated in a single path and row over lap zone (170 and 56). On the other hand, actual and potential evapotranspiration were assessed using satellite images acquired by the Land Sat 8 operational land imager sensor (L8-OLIS) and then analyzed using the ENVI software.

**Evapotranspiration**

The loss of water from open water, soil, and plant surfaces was referred to as evapotranspiration (ET), and the ET is determined by the energy and heat exchanges that occur at the land surface. Furthermore, the land surface energy balance algorithm (SEBAL) was utilized to assess actual and projected evapotranspiration. In its most simple version, the surface energy balance algorithm for land, omitting the energy necessary for photosynthesis and heat retention in plants, is as follows [12]:

$$\lambda ET = Rn - Go - H \quad (1)$$

where $Rn$ denoted the net radiation absorbed at the land surface $(W/m^2)$, and $Go$ represented the soil heat flux to warm or cool the soil ($W/m^2$); $H$ represented the sensible heat flux to warm or cool the atmosphere ($W/m^2$), and $ET$ represented the latent heat flux associated with evaporation of water from soil, water, and vegetation ($W/m^2$). Moreover, a physically-based one-layer sensible heat transfer system and an experimental estimation system for soil heat flux are combined in the practical SEBAL method. Surface temperature, surface albedo, and the normalized vegetation index (NDVI) were used as dependent variables to calculate the soil heat flux as an empirical fraction of net radiation. Then, the net radiation was calculated using radiation's spatially variable reflectance and emittance. Net radiation (Rn) was calculated as the sum of inward and outward radiation components.Net short-wave radiation was calculated using astronomical equations and estimates of atmospheric transmittance ($\tau_{sw}$) and $\alpha_0$, incoming long wave radiation was modeled using overpass time and air temperatures (Ta), which were assumed to be constant over the area.

CC BY NC ND

ajfand SCHOLARLY, PEER REVIEWED AFRICAN JOURNAL OF FOOD, AGRICULTURE, NUTRITION AND DEVELOPMENT Volume 22 No. 7 September 2022 PUBLISHED BY AFRICAN SCHOLARLY SCIENCE COMMUNICATIONS TRUST ISSN 1684 5374

Surface temperature (Ts) and an estimate of surface emissivity (Ɛo) on the basis of NDVI were used to calculate outgoing long-wave radiation. Sensible heat flux (H) was also the rate of heat loss to the air due to temperature variations via convection and conduction. Sensible heat flux (H) was calculated using the air density fraction, specific heat constant, temperature difference, and aerodynamic resistance. The energy budget is closed on a pixel-by-pixel basis by using λET as the residual of the energy budget equation. To determine its constitutive parameters, this method requires spectral radiance in the visible, near infrared, and thermal infrared regions of the spectrum: surface albedo ($\alpha_0$), NDVI, and surface temperature (Ts).

$$\mathbf{R_n = (1-\alpha)R_s\downarrow + R_L\downarrow - R_L\uparrow - (1-\varepsilon_0)\,R_L\downarrow} \quad (2)$$

where, $R_s\downarrow$ is the incoming short-wave solar radiation, $\alpha$ is the surface short-wave albedo, $R_L\downarrow$ and $R_L\uparrow$ are incoming and outgoing long-wave radiation (W/ $m^{-2}$ ), $\varepsilon o$ is the land surface emissivity. Standard algorithms and/or land surface parameterization schemes are used to calculate all of this.

Surface albedo was defined as the ratio of solar electromagnetic radiation reflected from soil and plant surfaces to incoming radiation. Its value was calculated by combining the spectral reflectance values from Landsat 8 OLI's visible, near-infrared, and short-wave bands [13]. The surface albedo was calculated using the following equation:

$$\alpha = \frac{\alpha_{toa} - \alpha_{path-radiance}}{\tau_{sw}^2} \quad (3)$$

where α _path radiance was the average of the fraction of solar incident radiance scattered to the sensor before reaching ground level for all bands. Its values range from 0.025 to 0.04, with 0.03 recommended for SEBAL [11]. Furthermore, τsw was the atmospheric transmissivity, which was calculated using equation (4):

$$\mathbf{\tau_{sw} = 0.75 + 2 * 10^{-5} * Z} \quad (4)$$

where, Z was the height of the meteorological station from the mean sea level[12]. Surface albedo was computed by correcting the ($\alpha_{toa}$) atmospheric transmissivity. The simplest method was proposed by Liang [3].

$$\alpha_{toa} = \frac{0.356\rho_2 + 0.130\rho_4 + 0.373\rho_5 + 0.085\rho_6 + 0.072\rho_7 - 0.0018}{0.356 + 0.130 + 0.373 + 0.085 + 0.072} \quad (5)$$

whereas, $\rho_2$, $\rho_4$, $\rho_5$, $\rho_6$, $\rho_7$ band (2, 4, 5, 6 and 7) respectively from landsat8 image analysis. According to the Liang [17], band$_3$ was ignored during the evaluation of surface albedo (the green part of the spectrum).

CC BY NC ND

ajfand SCHOLARLY, PEER REVIEWED AFRICAN JOURNAL OF FOOD, AGRICULTURE, NUTRITION AND DEVELOPMENT Volume 22 No. 7 September 2022 PUBLISHED BY AFRICAN SCHOLARLY SCIENCE COMMUNICATIONS TRUST ISSN 1684 5374

The flux of direct and diffuse solar radiation that actually reaches the ground, assuming clear sky conditions, for the incoming short-wave radiation was calculated as the following equation [14] :

$$R_s\downarrow = S_c \cos\theta * d_r * \tau_{sw} \quad (6)$$

$S_c$ denoted the solar constant, which is equal to 1367 ($W/m^2$). Cosθ was the cosine of the incident angle of solar radiation, which can be found in the satellite image header file (for Landsat8 data in OLI format). dr was calculated as the inverse of the square relative distance of the Earth to the Sun [ 14]:

$$d_r = 1 + 0.033 \cos\left(\frac{2\pi}{365} J\right) \quad (7)$$

where; J was the sequential day of the year.

The reflected long-wave radiation flux is calculated using Stefan-Boltzmann's relation as:

$$R_L\uparrow = \varepsilon_o \sigma T_s^4 \quad (8)$$

where, $\varepsilon_0$ was the broadband surface emissivity, σ was the Stefan-Boltzmann constant ($5.67 \times 10^{-8}$ $W/M^2/K^4$) and $T_s$ was the surface temperature (K) evaluated using ENVI software researcher was analyzed Land Sat 8 image [15].

The following equation was used to calculate the broad band surface emissivity:

$$\varepsilon_o = 0.004 * pv + 0.986 \quad (9)$$

$$pv = \left(\frac{NDVI - NDVI_{\min}}{NDVI_{\max} - NDVI_{\min}}\right) \wedge 2 \quad (10)$$

where, NDVI normalized difference vegetation index, $NDVI_{min}$ was normalized difference vegetation index at minimum condition, $NDVI_{max}$ was normalized difference vegetation index at maximum condition and pv was proportion of vegetation.

NDVI was calculated as the following equation [14].

$$NDVI = \frac{\rho_5 - \rho_4}{\rho_5 + \rho_4} \quad (11)$$

where; $\rho 5$, $\rho 4$ were the spectral band 5, and band 4, respectively.

Incoming longwave radiation ($R_L\downarrow$) radiation was the flux of thermal radiation from the atmosphere downwards, which was calculated using the Stefan-Boltzmann equations:

$$R_L\downarrow = \varepsilon_a \sigma T_a^4 \quad (12)$$

CC BY NC ND

ajfand SCHOLARLY, PEER REVIEWED AFRICAN JOURNAL OF FOOD, AGRICULTURE, NUTRITION AND DEVELOPMENT Volume 22 No. 7 September 2022 PUBLISHED BY AFRICAN SCHOLARLY SCIENCE COMMUNICATIONS TRUST ISSN 1684 5374

where; $T_a$ was the temperature of the air near the surface, and $\varepsilon_a$, atmospheric emissivity [16]. The following equation was used to calculated atmospheric emissivity:

$$\varepsilon_a = 0.85(-\ln \tau_{sw})^{0.09} \quad (13)$$

Soil heat flux needed in SEBAL algorithm cannot be calculated directly from satellite images. Therefore, an mathematical equation was applied to estimate Go, which utilizes *NDVI* and Rn. The equation was

$$G_o = \left(0.30\left(1-0.98NDVI^4\right)\right)R_n \quad (14)$$

This equation was derived from actual measurements as reported in [12]. Some publications claim that Equation (14) was only applied to a vegetated land surface [17]. Sensible heat flux was the rate of heat loss to the air by convection and conduction due to a temperature difference. The classical expression for sensible heat flux was a function of the temperature gradient, surface roughness and wind speed and this step has high propensity to failures in the process due to considerations and assumptions. The sensible heat flux is represented by the Equation (15):

$$H = \frac{\rho_a c_p dT}{r_{ah}} \quad (15)$$

where $\rho_a$=air density kg $m^{-3}$; $C_p$=specific heat of air at constant pressure J $kg^{-1}$ $K^{-1}$; and $r_{ah}$=aerodynamic resistances $m^{-1}$between two near-surface heights, $z_1$ and $z_2$ generally 0.1 and 2m computed as a function of estimated aerodynamic roughness of the particular pixel. The dT parameter ($k^0$) represents the near-surface temperature difference between $z_1$ and $z_2$.

Allen postulated a linear relationship between dT and Ts, while others utilized a step function to calculate Ta from Ts values [18, 19]. This study performed a regression analysis using the *Ta* values available from the site meteorological stations and the radiometric LST provided from landsat8 image product. The resulting linear equation for the whole irrigation season is the following [20]:

$$dT(K^0) = -146.7055 + 0.5064T_s(K^0) \quad (16)$$

where, $Ts(k^0)$ was surface temperature, dT was temperature difference at pixel.
The vertical limits for specifying sensible heat flux (H) and near-surface vertical air temperature difference were defined as reference heights ($Z_1$ and $Z_2$, usually 0.1 and 2.0 m above ground, respectively) ($dT_a$). The sensible heat transfer equation makes these limits relevant to aerodynamic resistance ($r_{ah}$), [19]. By this approach ($r_{ah}$) was calculated as using the following equation [21]:

CC BY NC ND

$$r_{ah} = \frac{\ln\left(\frac{Z_2}{Z_1}\right)}{u * k} \quad (17)$$

where ($z_2/z_1$) denoted the reference height ($z_2/z_1$), k denoted the von Karmans constant (0.41), and u* denoted the fraction velocity.

The friction velocity (u*) at each pixel was calculated using observed wind speed measurements and the assumption that the wind speed at blending height was aerially constant (200m). Friction velocity (u*) was calculated using the equation:

$$u* = \frac{k u_{200}}{\ln\left(\frac{200}{Z_{om}}\right)} \quad (18)$$

where, $u_{200}$ was the wind speed at the blending height (200 m), k was the von karmans constant (0.41) and $z_{om}$ was the length of surface roughness for momentum transport. $u_{200}$ is the wind speed at an assumed blending height of 200 m above the weather station [22] .

$$u_{200} = \frac{u_y \ln(67.8Z - 5.42)}{4.87} \quad (19)$$

where, $u_{200}$(m/s) was the wind speed at blending height of 200m, $u_y$ (m/s)was wind speed at the observed from weather station at 2m and z (m) was the elevation above sea level close to weather station.

The initial estimate of surface roughness length for momentum transport ($Z_{om}$) in the SEBAL method is based on the height of vegetation around the weather station (h) using an empirical equation [23].

$$Z_{om} = 0.12h \quad (20)$$

The evaporative fraction (Λ) converts the instantaneous flux values determined above for the satellite overpass time to daily and average monthly evaporation rates.

$$\Lambda = \frac{\lambda ET}{R_n - G_o} \quad (21)$$

According to the literature, the instantaneous evaporative fraction is equivalent to the 24 h evaporative fraction and is used to compute potential evaporation from instantaneous latent heat fluxes [24]. The instantaneous SEBAL output may then be

CC BY NC ND

used to determine actual and prospective evapotranspiration [25].The potential condition ( $\lambda ET_p$)[26] was used to determine the latent heat flows shown below.

$$\lambda ET_p = R_n - G_o \quad (22)$$

**Performance indicators**

Based on observed flows of water at various points in the water application system, irrigation performance indicators have been expressed in terms of efficiency. According to Bastiaanssen, the overall consumed ratio (ep) is defined as the ratio of the volume of irrigation water required and made available for crop evapotranspiration during the growth cycle ($m^3$) to the volume of water directed to the field [27, 28].The total water supply at the irrigation system level is the total amount of water flowing into the domain from precipitation plus any irrigation supply from diversion. Crop demand is calculated using potential evapotranspiration (ETp) under well-watered conditions. As a result, ep can be estimated from:

$$e_p = \frac{ET_p - p_e}{v_c} \quad (23)$$

where (ep) is the overall consumption ratio, (ETp) is the potential evapotranspiration, (Pe) is the effective precipitation, and vc is the volume of water that diverted from source to the commend area. If the supply is adequate, the ep value will be around 1.0. If this value is greater than 1.0, it indicates under-irrigation; if it is less than 1.0, it indicates over-irrigation.

During periods of low ratio, the non-consumed fraction of the water causes the groundwater table to rise (only if this water is applied to the field; during high ratio periods, groundwater must be pumped) [29].

Actual evapotranspiartion (ETa) and potential evapotranspiration (ETp) values in this equation were derived from satellite RS. Field measurements and Omo Kuraz Sugar Development Meteorology Station records were used to calculate Vc and Pg. Pe was calculated using the CROPWAT8.0 software.

It should be noted that this ratio (ep) does not reflect whether the crop received the appropriate amount of water at the appropriate time, but rather it highlights the overall situation of water supply and demand. The ratio does not also indicate how efficiently the water supply was used.

In water-stressed conditions, depleted fraction (DF) is more important and is defined as the adequate amount of water added to crop at the correct time. The following

CC BY NC ND

equation was used to compute DF, which refers to the ratio of actual evapotranspiration (ETa) to the amount of water added to the field, as reported by Bandara [30]:

$$DF = \frac{ET_a}{v_c + p_g} \tag{24}$$

where ETa is actual evapotranspiration, Vc is the volume of water diverted to the commend area, Pg is gross precipitation, and beneficial depletion is considered because a plant cannot transpire without soil evaporation. The critical value of the depleted fraction in semi-arid and arid regions ranges between 0.5 and 0.7 (average around 0.6) [31]. If ETa is less than about 0.6(Pg+Vc), a portion of this available water goes into storage, causing the groundwater table to rise, whereas storage decreases if ETa is greater than 0.6(Pg+Vc) [31].

The depleted fraction does not indicate an equal distribution of water in an irrigated agricultural field, whereas the evaporative fraction is more important in terms of equity or uniformity of water that is distributed to crops according to their needs, as expressed by the following expression:

$$\Lambda = 1 - \frac{H}{R_n - G_o} \tag{25}$$

Unlike the evaporative portion, Rn net radiation, H sensible heat flux, and Go soil heat flux are all positive. Evaporative fraction values of 0.8 or higher indicate no stress, while values below 0.8 indicate increased moisture shortage to meet crop water requirements due to inadequacy water supplies [32].

The evaporative fraction does not reflect whether or not water is applied in the area at the appropriate time. Relative evapotranspiration is a good indicator parameter for determining the dependability of a water application because it detects water-short areas. As demonstrated by Bandara and Bos[31, 30], the following equation was used to calculate it:

$$RET = \frac{ET_a}{ET_p} \tag{26}$$

where RET refers to relative evapotranspiration, ETa stood for actual evapotranspiration, and ETp stood for potential evapotranspiration. A RET of ≥ 0.75 was very well acceptable for irrigated agriculture during the growing season, though this does not remain constant over time. The crop yield response factor relates relative evapotranspiration to relative yield changes as the crop progresses through its phenological stages [33].

CC BY NC ND

ajfand SCHOLARLY, PEER REVIEWED AFRICAN JOURNAL OF FOOD, AGRICULTURE, NUTRITION AND DEVELOPMENT Volume 22 No. 7 September 2022 PUBLISHED BY AFRICAN SCHOLARLY SCIENCE COMMUNICATIONS TRUST ISSN 1684 5374

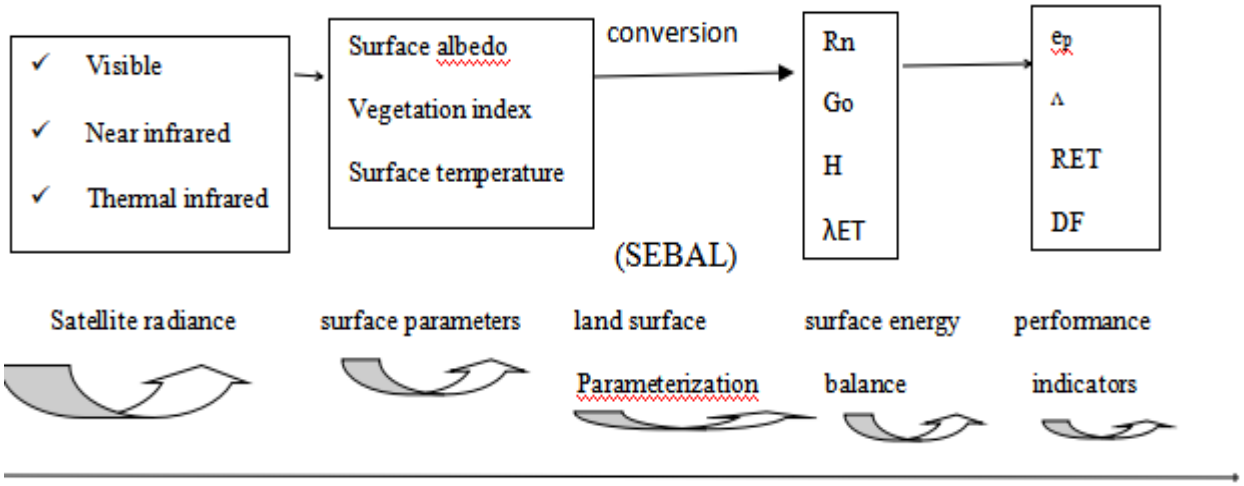


**Figure 2: Flowchart of the research**

## RESULTS AND DISCUSSION

### Data used in calculation of irrigation performance indicators

Table 1 shows the monthly and seasonal values of the Vc, Pg, and Pe parameters required to calculate the selected irrigation performance indicators for the 2018-2019 irrigation season. The amount of water that was delivered to the field within the two seasons was recorded by using staff gauge for one year. The amount of discharge calculated as m3/s was converted to millimeter (mm). Tables 2 and 3 show monthly and seasonal values of the ETa and ETp parameters required to calculate irrigation performance indicators for the 2018-2919 irrigation seasons. Sugar cane was the dominant crop on the Omo Kuraz sugar cane development project site. Table 4 shows the crop areas for the 2018-2019 irrigation seasons at each experimental site. The total area of these sugar cane plantations and surface irrigation system was carried out with reference to the sugar cane. ETa and ETp values vary among pixels in tables 2 and 3 due to crop pattern variation, vegetative growth, and poor irrigation water operation. Table 5 shows the results of irrigation system performance indicator parameter.

### Overall consumed ratio($e_p$)

Because the total water supply was the first measurement in an irrigation system, $e_p$ would be the first available indicator in each experimental area [27]. Table 5 shows the monthly values of the ep indicator for evaluating irrigation performance.

The following ep indicator values were obtained: TP (0.6, 0.6, 0.5 0.6) October, January, April, and July values, TE (0.6, 0.7, 0.3, 0.6) October, January, April, and July values, TM (0.6, 0.6, 0.4, 1) October, January, April, and July values, and TH (0.5, 0.6, 0.8, 0.6) October, January, April, and July values, respectively. Some treatment sites

CC BY NC ND

yielded extremely high results, while others yielded negative results, indicating that ETP was less effective than effective precipitation. This condition developed as a result of excessive water delivered from the source to the agricultural field. The highest ep values for all treatments were for (except TH of July) during the study period. Except for TH July, these values were less than the target value (1). This result demonstrates that in all treatments, monthly irrigation water application necessitates the use of some irrigation management technique.

Table 5 shows the seasonal values and temporal variation of the ep indicator. The overall treatment's average seasonal ep indicator was less than the target value of 1. This is a clear indication that the water application technique was ineffective for all treatments. The results show that all treatments indirectly raised the groundwater table the most and had the poorest performance with the lowest ep value. This could be influenced by the fact that there was unscheduled irrigation application and the systems' poor operational performance. Because of the relatively balanced approach, there is a spatial variation in the irrigation system's efficiency in the July Tm experimental field. This was supported by the crop's relatively good efficient performance value (1), which limited some extra water percolation to the root zone. This entire treatment (Tp, TE, TM, TH) must use scheduled irrigation application, and thus its irrigation application induced some water flow to the field. Thus, Omo sugar project was unable to harvest crop on time due to drainable surplus water. As a result, the crop grew over a long period of time in the area. From an economic standpoint, the system was inefficient. As a result, irrigation agronomists must avoid irrigating the crop, particularly in April close to the harvest time in order to keep the water content in the cane as low as possible.

During periods with low ratios, meaning that the overall consumed fraction of water was shown in all experimental sites, some extra water added to the field that was not consumed by the crop caused the groundwater table to rise [6]. During times when the ratio is close to 0.6, groundwater must be pumped out from agricultural field and irrigation water management techniques must be used to solve the drainage problem.

The $e_p$ indicators vary from month to month due to variations in monthly water requirements, effective precipitation, and water volume obtained. As a result, all treatment sites in the study experienced increased irrigation problems during the 2018-2019 irrigation seasons. However, the average ep values of all of the experimental sites of the project area were experiencing excess water supply and this induced surface drainage problems. Reported results from another study, the seasonal averages of the ep of Gediz, Sarikiz, Mesir, and Turgutlu water use associations in the lower Gediz Basin were 0.56, 0.0.9, 0.8, and 0.81, respectively, for the 2004 irrigation season [34]. These

CC BY NC ND

values are comparable to the monthly results obtained in this study across all treatments.

**Depleted fraction (DF)**

A critical value of DF (0.6) indicates that if ETa is less than about 0.6 (Pg + Vc), a portion of the water applied to the field raises the groundwater table, causing the agricultural field drainage problem. In contrast, crop water requirements increase if ETa is greater than 0.6 (Pg + Vc). Table 5 shows the monthly values of the DF indicator for evaluating irrigation performance. As shown in Table 5, there are no values of the DF indicator for all treatments at the planting, early, middle, and harvesting stages (TP, TE, TM, TH) good performance, some unnecessary water added to the field, so it must be safely avoided from the field. Except in one case, the averages of DF values for all Ts in an Omo Kuraz irrigation project area were ETa less than the critical value (0.6 (Pg+Vc)). In this study (Tm) July has a relatively safe water dose in the study area, but results from other experimental sites show that the unused portion of water delivered from the source in these remaining months may feed the groundwater. A large amount of extra water was delivered from a nearby source, but the plants consumed nearly as much water, while the excess water had to be removed from the site.

Because the researcher observed the field treatment site on the furrow using auger in the different root depth in all treatment areas until one meter there is soil moisture, indicating that extra water was supplied, the DF results of all treatments were especially low in $T_M$ on July, indicating that much more water was applied. This value may be influenced by a poor irrigation system, which may cause the groundwater table to rise. The monthly DF values for all treatments were far below the critical value indicating that a significant portion of the water delivered from the source during these months (except for $T_M$ July) could not have been consumed by the plants. This observation could explain the irrigation system's inadequacy. According to the findings of this study, adequacy is defined as a closed approached value from both the upper and lower parts of the number (0.6(vc+pg)) to ETa, because less than ETa and greater than ETa in both conditions indicate that the irrigation system is inadequate. In the case of the first condition, if 0.6(vc+pg) is less than ETa, a drainage problem has occurred, and some irrigation water management is required. If 0.6(vc+pg) is greater than ETa, the crop is under water stress and requires additional water application. Adequacy was related to crop water requirement and anything above or below crop water requirement was inadequacy.

Except for TM July, the performance of all treatments is within acceptable limits. As determined by the other performance indicators in Table 5, this result can be attributed

CC BY NC ND

to irrigation water application and poor irrigation water management. Values for diverted water were quite high for all treatments, and DF values fluctuated erratically, indicating that neither good operation nor good water application had been achieved.

Menemen LB Water Use Association conducted a study in the Gediz Basin and discovered DF values of 0.60 and 0.72 for cotton and grapes respectively [35]. The seasonal value for this water use association was found to be 0.6 in this study, which did not differentiate between crops. This value is consistent with the findings of another study [28]. In that study of the Nilo Coelho irrigation system, it was reported the average DF values of 0.6. Except for Salihli RB and Salihli LB, this value was lower than the seasonal average values of the DF indicator. Furthermore, seasonal averages of DF for the same basin's Sarigol, Bag, and Uzum WUAs were found to be 0.53, 0.59, and 0.68, respectively [36]. These values are nearly identical to the monthly values identified in this study.

**Evaporative fraction**

Table 5 shows the monthly values of the evaporative fraction(ʌ) indicator. Monthly values were above allowable levels (>0.8 indicates no stress and <0.8 inadequate), but Allen's statement (≤ 0.8 indicates no stress and ≥ 0.8 reflects increases in moisture shortage) was not a valid argument because the parameter related to soil heat flux was inversely related [1,32]. In this study, above the critical value (0.8), the crop was not under water stress, and numerical variation within the same stage indicates that water distribution varied. In general, during surface irrigation methods, equity was under requirement or simply not achievable from a crop standpoint. Because there is no equity if you add more water than the crop requires or less water than the crop requires. While all Ts, with the exception of October, showed water distribution within acceptable limits, there was no equal or uniform distribution of water to meet crop water requirements.

Table 5 displays the monthly values of ʌ indicators. Every treatment site's monthly value exceeded the critical limit evaporative fraction. However, if the total crop water requirements (ETp) in Table 3 were evaluated alongside total monthly values of potential evapotranspiration (ETp), it can be stated for all Ts that approximately some water not consumed by the crop was percolated to ground water. A lack of month-to-month consistency in the ʌ indicator can also be seen in the values (Table 5). However, it is clear that it exhibited the same homogeneity variation across three performance indicators. A study on the Omo kuraz sugar cane development irrigation system in Ethiopia [11] showed ʌ values in the range of 0.7-0.9. According to Bastiaanssen, this was a direct result of keeping the top soil moist through irrigation and having a nearly complete crop cover. These findings led to the conclusion that the evaporative fraction

CC BY NC ND

was a direct and straightforward indicator of root zone soil moisture condition in general. According to the findings of this study, the monthly value ʌ indicators for all treatments were within critical limits. Another study found that the monthly value of during an earlier mango energy balance study in 1998 was 0.73 in August, 0.86 in September, 0.78 in October, and 0.80 in November, although these values are comparable to the monthly value obtained in this study [37, 38]. Lotufo stated that an evaporative fraction (ʌ) value of around 0.83 corresponded to a 67 percent degree of soil moisture saturation in the root zone, which is consistent with our arguments [39].

**Relative Evapotranspiration (RET)**

Table 5 shows the monthly values of the RET indicator. All treatments had the highest RET values in January and July. This is because there is very little variation in the monthly sensible heat flux. The majority of sugar cane leaves were covered in moisture during marring between January and July, resulting in the highest sensible heat flux. In this study, all treatment RET values were greater than the critical limit. RET is the ratio of actual to potential evapotranspiration. Relative Evapotranspiration (RET) values: Tp (0.9, 0.8, 0.8, 0.8) in October, January, April, and July, respectively. Other values, such as TE, TM, and TH, were also the same as the Tp values mentioned above. This result was reflected in the recommended value for the study area's irrigated agricultural land (Table 5) [5]. As a result of this, the indicator RET critical value indicates good performance. According to Bastiaanssen, the operational range is 0.8 to 1 and the acceptable range is 0.7 to 1[28]. The findings from the current study are consistent with this recommendation. The above result indicates that the irrigation system in the study area has been consistently reliable. As a result, the monthly RET performance of all treatments was typically good. The values obtained from the study area also show the temporal variation of RET indicator (Table 5).

The average value of RET in the Nilo Coelho irrigation system in Brazil was determined using remote sensing to be 0.7, 0.76, and 0.8 [28]. Even though the RET averages for the treatments (T) in the study area were greater than 0.75, indicating that the system was reliable under water stress conditions, it was not applicable under water excess conditions. As stated previously, three indicator results show extra water found in the agricultural field, implying that they had a greater problem with water supply. Though these arguments are similar to the monthly averages obtained in the current study, they are typically worse than those of the majority of Ts.

## CONCLUSION

According to data from the operation of the four experimental sites in the Lower Omo Basin, including the Omo Kuraz irrigation site, the spatio-temporal patterns of the

CC BY NC ND

irrigation system performance indicators under the four pillars of effectiveness, sufficiency, reliability, and equity were shown in (table 5). Satellite data allow for the recovery of new performance pillars such as the overall consumed ratio (ep), depleted fraction (DF), evaporative fraction, and relative evapotranspiration. Each pillar has its own set of irrigation system performance indicator parameters (efficiency, adequacy, reliability, and equity).

Irrigation system performance for all treatments, whether taken monthly or seasonally, was typically poor. In terms of the variability of monthly performance indicator values, supplied water values to the field were generally very high, indicating that irrigation was not uniform across the months. This result was attributed to the fact that the effective precipitation was not taken into account by the workers who irrigated the crop. In order to manage subpar irrigation system performance, irrigation scheduling based on crop water requirements was successfully carried out. Each experimental site had a slightly different performance indicator calculated using the four pillars. The primary cause of this poor performance is unscheduled crop water requirements. Because irrigation agronomists did not normally take into account resident soil moisture during irrigation, the workers did not know the accurate water dose to apply to the crop.

The irrigation system was inefficient, as evidenced by the low overall consumed ratio. This was due to an excess of water supplied to the field. Similarly, the deflated fraction result showed some excess water-induced percolation to the groundwater. These results suggests that the irrigation system was inadequate and hence any additional water should be drained from the field to sustain the project. Gorantiwar [7] states that evaporative fraction values of $\leq 0.8$ indicate no stress and those of $\geq 0.8$ indicate an increase in moisture stress. These findings, however, contradict the preceding argument. The moisture condition of the field soil before and after irrigation, as well as crop root depth, were measured. When a soil auger was used in each experimental site, there was no indication of soil moisture stress. On the other hand, the results in Table5 show that evaporative fraction value was $\geq 0.8$, indicating that there was no moisture stress even though the irrigation system had plenty of water. In general, the irrigation system performance indicator parameter indicates that the Omo Kuraz irrigation system performed poorly.

To improve irrigation system performance, the period when water is demanded from the source and the period when the crop requires water should coincide completely. Additionally, irrigation scheduling is necessary because water delivery to fields must be carefully planned in accordance with crop water requirements and its growth stage.

CC BY NC ND

ajfand SCHOLARLY, PEER REVIEWED
AFRICAN JOURNAL OF FOOD, AGRICULTURE, NUTRITION AND DEVELOPMENT
Volume 22 No. 7
September 2022
PUBLISHED BY AFRICAN SCHOLARLY SCIENCE COMMUNICATIONS TRUST
ISSN 1684 5374

**ACKNOWLEDGEMENTS**

The authors would like to acknowledge the financial assistance received from the Omo Kuraz irrigation development office that was used in carrying out this study. Data collection was funded by Arbamich University. We also thank the Wolayita Sodo University and Arbamich University for sponsoring the publication. The authors would also like to acknowledge the support of Dr. Getachew who helped with language editing and proofreading of this article. We further thank the officials for good work in data collection and most importantly to irrigation agronomists who patiently gave us their time and responded to our questions.

CC BY NC ND

ajfand SCHOLARLY, PEER REVIEWED AFRICAN JOURNAL OF FOOD, AGRICULTURE, NUTRITION AND DEVELOPMENT Volume 22 No. 7 September 2022 PUBLISHED BY AFRICAN SCHOLARLY SCIENCE COMMUNICATIONS TRUST ISSN 1684 5374

**Table 1: Amount of the water diverted from source (*V*c), total precipitation (*P*g) and effective precipitation (*P*e) parameters needed to calculate performance indicators during the 2018-2019 irrigation season**

| Treatment(T) | Water diverted from regulator, Vc(mm) | | | | |
|---|---|---|---|---|---|
| | Oct | June | April | July | total |
| TP | 258 | 298 | 102 | 256 | **914** |
| TE | 274 | 285 | 170 | 220 | **949** |
| TM | 281 | 300 | 114 | 114 | **809** |
| TH | 270 | 313 | 64 | 213 | **860** |
| Pg(mm) | 27.3 | 0 | 285.3 | 48.3 | **360.9** |
| Pe (mm) | 26.1 | 0 | 153.5 | 44.6 | **224.2** |

**Table 2: Values of monthly and seasonal actual evapotranspiration (ETa) during the 2018-2019 irrigation season**

| Treatment(T) | ETa(mm) | | | | |
|---|---|---|---|---|---|
| | Oct | Jan | April | July | total |
| TP | 168 | 172 | 177 | 168 | 685 |
| TE | 174 | 169 | 170 | 150 | 663 |
| TM | 180 | 172 | 172 | 156 | 680 |
| TH | 171 | 168 | 177 | 156 | 672 |
| Average (mm) | **173** | **170** | **174** | **158** | **675** |

CC BY NC ND

ajfand SCHOLARLY, PEER REVIEWED AFRICAN JOURNAL OF FOOD, AGRICULTURE, NUTRITION AND DEVELOPMENT Volume 22 No. 7 September 2022 PUBLISHED BY AFRICAN SCHOLARLY SCIENCE COMMUNICATIONS TRUST ISSN 1684 5374

**Table 3: Values of monthly and seasonal potential evapotranspiration (ETp) during the 2018-2019 irrigation season**

| Treatment(T) | ETp(mm) | | | | |
|---|---|---|---|---|---|
| | Oct | June | April | July | total |
| TP | 187 | 215 | 221.2 | 210 | 833.2 |
| TE | 193 | 211 | 212 | 187 | 803 |
| TM | 211 | 144 | 144 | 129 | 628 |
| TH | 192 | 210 | 223 | 197 | 822 |
| Average (mm) | **196** | **199** | **200** | **181** | **771** |

**Table 4: Crop area for the 2018-2019 irrigation season in all experimental site**

| Crop | TP(ha) ) | TE(ha) | TM(ha) | TH (ha) |
|---|---|---|---|---|
| Sugar cane | 27.25 | 27.884 | 15.11 | 34.02 |

Source: General Directorate of the Omo Kuraz sugar cane development research office (OKSR 2018-2019)

CC BY NC ND

ajfand SCHOLARLY, PEER REVIEWED
AFRICAN JOURNAL OF FOOD, AGRICULTURE, NUTRITION AND DEVELOPMENT
Volume 22 No. 7
September 2022
PUBLISHED BY AFRICAN SCHOLARLY SCIENCE COMMUNICATIONS TRUST
ISSN 1684 5374

**Table 5: Monthly value of performance indicators for all treatment during the irrigation seasons were**

| Treatment | Overall consumed ratio (EP) | | | | Depleted fraction (DF) | | | | Evaporative fraction (Λ) | | | | Relative evapotranspiration (RET) | | | |
|---|---|---|---|---|---|---|---|---|---|---|---|---|---|---|---|---|
| | Oct | Jan | Apr | Jul | Oct | Jan | Apr | Jul | Oct | Jan | Apr | Jul | Oct | Jan | Apr | Jul |
| TP | 0.6 | 0.6 | 0.6 | 0.6 | 0.58 | 0.57 | 0.45 | 0.54 | 0.91 | 0.85 | 0.85 | 0.84 | 0.9 | 0.8 | 0.8 | 0.8 |
| TE | 0.6 | 0.7 | 0.3 | 0.6 | 0.57 | 0.59 | 0.37 | 0.55 | 0.9 | 0.84 | 0.84 | 0.81 | 0.9 | 0.8 | 0.8 | 0.8 |
| TM | 0.6 | 0.6 | 0.4 | 1 | 0.58 | 0.57 | 0.4 | 0.96 | 0.91 | 0.84 | 0.84 | 0.82 | 0.90 | 0.8 | 0.8 | 0.8 |
| TH | 0.5 | 0.6 | 0.8 | 0.6 | 0.57 | 0.53 | 0.5 | 0.59 | 0.9 | 0.85 | 0.85 | 0.82 | 0.9 | 0.8 | 0.8 | 0.8 |
| **Total** | **2.3** | **2.5** | **2.1** | **2.8** | **2.3** | **2.26** | **1.72** | **2.64** | **3.62** | **3.38** | **3.38** | **3.29** | **3.6** | **3.2** | **3.4** | **3.8** |

CC BY NC ND

## REFERENCES


1. **Perry C, Steduto P, Allen RG and CM Burt** Increasing productivity in irrigated agriculture: Agronomic constraints and hydrological realities. Agricultural Water Management. 2009; **96(11):** 1517-1524.

2. **Nageswara Rao PP and A Mohankumar** Cropland inventory in the command area of Krishnarajasagar project using satellite data. *International journal of remote sensing*. 1994; ***15*(6)**: 1295-1305.

3. **Stone LR, Schlegel AJ, Gwin Jr RE and AH Khan** Response of corn, grain sorghum, and sunflower to irrigation in the High Plains of Kansas. Agricultural Water Management. 1996; **30(3):** 251-259.

4. **Murthy R, Dougherty PM, Zarnoch SJ and HL Allen** Effects of carbon dioxide, fertilization, and irrigation on photosynthetic capacity of loblolly pine trees. Tree Physiology. 1996;**16(6):** 537-546.

5. **Rao PS** Review of selected literature on indicators of irrigation performance. Iwmi. 1993; 41-43

6. **Wolters W, Zevenbergen AW and MG Bos** Satellite remote sensing in irrigation. *Irrigation and Drainage Systems*. 1991; ***5*(4):** 307-323.

7. **Gorantiwar SD and IK Smout** Performance assessment of irrigation water management of heterogeneous irrigation schemes: 1. A framework for evaluation. Irrigation and Drainage Systems. 2005; **19(1):** 1-36.

8. **Molden DJ and TK Gates** Performance measures for evaluation of irrigation-water-delivery systems. Journal of irrigation and drainage engineering. 1990; **116(6):** 804-823.

9. **Engman ET and R Gurney** Recent advances and future implications of remote sensing for hydrologic modeling. **In**: Recent advances in the modeling of hydrologic systems. 1991; (pp. 471-495).

10. **Thiruvengdachari S** Remote Sensing in Water Resources. Training Course in Water Resources. NRSA: Hyderabad, India. 1993.

11. **Bastiaanssen WGM** SEBAL-based Sensible and Latent Heat Fluxes in the Irrigated Gediz Basin, Turkey. Journal of hydrology. 2000; **229(1):** 87-100.


CC BY NC ND

12. **Bastiaanssen WGM, Menenti M, Feddes RA and AAM Holtslag** A Remote Sensing Surface Energy Balance Algorithm for Land (SEBAL): Part 1: Formulation. Journal of hydrology, (1998a) 212, 198-212.

13. **Allen RG** Using the FAO-56 dual crop coefficient method over an irrigated region as part of an evapotranspiration intercomparison study. *Journal of hydrology*. 2000b; ***229*(1-2):** 27-41.

14. **Allen RG, Tasumi M and R Trezza S**urface energy balance algorithms for advanced training and user manual. a NASA EOSDIS/Synergy grant from the Raytheon Company through The Idaho Department of Water Resources. 2002; **133(4):** 380-394.

15. **Bastiaanssen WGM, Noordman EJM, Pelgrum H, Davids G, Thoreson BP and RG Allen** SEBAL model with remotely sensed data to improve water-resources management under actual field conditions. *Journal of irrigation and drainage engineering*. 2005; ***131*(1):** 85-93.

16. **Sun Z, Wei B, Su W, Shen W, Wang C, You D and Z Liu** Evapotranspiration estimation based on the SEBAL model in the Nansi Lake Wetland of China. *Mathematical and Computer Modelling*. 2011; ***54*(3-4):** 1086-1092.

17. **Li S and W Zhao** Satellite-based actual evapotranspiration estimation in the middle reach of the Heihe River Basin using the SEBAL method. *Hydrological Processes*. 2010; ***24*(23)**: 3337-3344.

18. **AllenRG, Tasumi M, Morse A, Trezza R, Wright JL, Bastiaanssen W and CW Robison** Satellite-based energy balance for mapping evapotranspiration with internalized calibration (METRIC)-Model. *Journal of irrigation and drainage engineering*. 2007a; **133(4):** 395-406.

19. **Farah HO and WG Bastiaanssen** Impact of spatial variations of land surface parameters on regional evaporation: a case study with remote sensing data. *Hydrological processes*. 2001; ***15*(9):** 1585-1607.

20. **Alexandridis TK, Cherif I, Chemin Y, Silleos GN, Stavrinos E and GC Zalidis** Integrated methodology for estimating water use in Mediterranean agricultural areas. *Remote Sensing*, (2009); ***1***(3): 445-465.

21. **Shoubo Li and Wenzhi Zhao**, Satellite- based actual evopotranspiration estimation in the middle reach of the Heihe River Basin using the SEBAL methods, (2010).

CC BY NC ND

22. **Allen RG, Pereira LS, Raes D and M Smith** Crop evapotranspiration-Guidelines for computing crop water requirements-FAO Irrigation and drainage paper 56. *Fao, Rome*. 1998; ***300*(9):** D05109.

23. **Waters R, Allen R, Bastiaanssen W, Tasumi M and R Trezza** Sebal. *Surface Energy Balance Algorithms for Land. Idaho Implementation. Advanced Training and Users Manual, Idaho, USA*. 2002; 9-28.

24. **Brutsaert W and D Chen** Diurnal variation of surface fluxes during thorough drying (or severe drought) of natural prairie. *Water Resources Research*. 1996;***32*(7):** 2013-2019.

25. **Bastiaanssen WG, Van der Wal T and TNM Visser** Diagnosis of regional evaporation by remote sensing to support irrigation performance assessment. Irrigation and Drainage Systems. 1996; **10(1):** 1-23.

26. **Mokhtari A, Noory H, Pourshakouri F, Haghighatmehr P, Afrasiabian Y, Razavi M and AS Naeni** Calculating potential evapotranspiration and single crop coefficient based on energy balance equation using Landsat 8 and Sentinel-2. *ISPRS Journal of Photogrammetry and Remote Sensing*. 2019; ***154*:** 231-245.

27. **Kazbekov J, Abdullaev I, Manthrithilake H, Qureshi A and K Jumaboev** Evaluating planning and delivery performance of water user associations (WUAs) in Osh Province, Kyrgyzstan. Agricultural water management. 2009; **96(8):** 1259-1267.

28. **Bastiaanssen WGM, Brito RAL, Bos MG, Souza RA, Cavalcanti EB and MM Bakker** Low cost satellite data for monthly irrigation performance monitoring: benchmarks from Nilo Coelho, Brazil. Irrigation and Drainage systems. 2001; **15(1):** 53-79.

29. **Wolff W** Wwolff7/SEBAL_GRASS. https://doi.org/10.5281/zenodo.167350

30. **Bandara Kmps** Assessing irrigation performance by using remote sensing, docoral thesis, Wageningen University, The Netherlands. 2006; p126.

31. **Bos MG, Burton MA and DJ Molden** *Irrigation and drainage performance assessment: practical guidelines*. CABI Publishing (2005).

32. **Bastiaanssen WG and MG Bos** Irrigation performance indicators based on remotely sensed data: a review of literature. *Irrigation and drainage systems*. 1999; ***13*(4):** 291-311.

CC BY NC ND

33. **Doorenbos J, and Kassam, A.H.** (1979) Yield response to water. FAO Irrigation and drainage paper, 33, 193p.

34. **Karatas BS, Akkuzu E, Unal HB, Asik S and M Avci** Using satellite remote sensing to assess irrigation performance in Water User Associations in the Lower Gediz Basin, Turkey. *Agricultural Water Management*. 2009; ***96*(**6): 982-990.

35. **Droogers P and W Bastiaanssen** Irrigation performance using hydrological and remote sensing modeling. *Journal of Irrigation and Drainage Engineering*. 2002; ***128*(1):** 11-18.

36. **Akkuzu E, Unal HB, Karatas BS, Avci M and S Asik** General irrigation planning performance of water user associations in the Gediz Basin in Turkey. Journal of irrigation and drainage engineering. 2007; **133(1):** 17-26.

37. **Teixeira ADC, Bastiaanssen WG, Moura MSB, Soares JM, Ahmad MUD and MG Bos** Energy and water balance measurements for water productivity analysis in irrigated mango trees, Northeast Brazil. Agricultural and forest meteorology. 2008; **148(10):** 1524-1537.

38. **Lotufo CM, Lopes C, Dubocovich ML, Farsky SH and RP Markus** Melatonin and N-acetylserotonin inhibit leukocyte rolling and adhesion to rat microcirculation. European journal of pharmacology**.** 2001; **430(2-3):** 351-357.

39. **Yepez EA, Williams DG, Scott RL and G Lin** Partitioning overstory and understory evapotranspiration in a semiarid savanna woodland from the isotopic composition of water vapor. Agricultural and Forest Meteorology. 2003; **119(1-2**): 53-68.

CC BY NC ND